Journal of
Materials Chemistry A

Accepted Manuscript

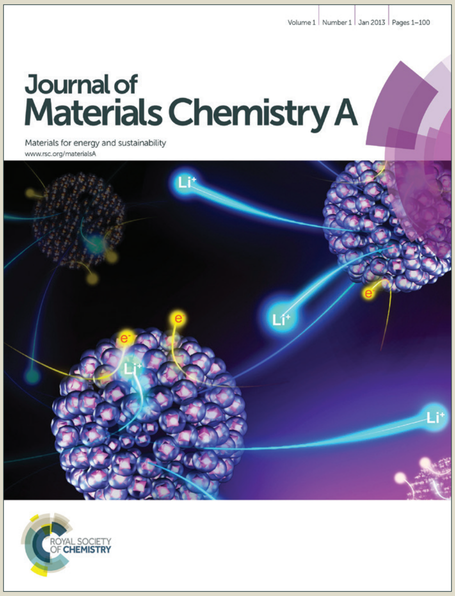

ROYAL SOCIETY
OF CHEMISTRY

www.rsc.org/materialsA

Journal of
Materials Chemistry A

RSCPublishing

ARTICLE

Cite this: DOI: 10.1039/x0xx00000x

Received 00th January 2012,
Accepted 00th January 2012

DOI: 10.1039/x0xx00000x

www.rsc.org/

Combining Palladium Complex and Organic Amine on Graphene Oxide for Promoted Tsuji–Trost Allylation

Qingshan Zhao, Yuanzhi Zhu, Zhen Sun, Yang Li, Guoliang Zhang, Fengbao Zhang, and Xiaobin Fan*

In this study, we develop a facile strategy to combine an organic amine with a palladium complex on graphene oxide (GO) as a cooperative catalyst for Tsuji–Trost allylation. The tertiary amine and palladium-diamine complex are simultaneously immobilized on the GO support through silylation and further in situ coordination processes. $PdCl_2$ is employed as the palladium precursor, with no necessary for extra coordination ligands. Various characterizations confirm the successful preparation of the cooperative supported catalyst (GO-NEt_2-2N-Pd). Systematic investigation reveals the immobilized palladium-diamine complex (GO-2N-Pd) with very low Pd-loading is effective for Tsuji–Trost allylation, and incorporation of the tertiary amine shows significantly promoted effect towards the catalytic activity. GO-NEt_2-2N-Pd can be readily recovered and recycled for several times without reduction of the efficiency. The excellent performance should be ascribed to synergistic catalysis effect, excellent support properties, and the robust immobilization interaction.

Introduction

Homogeneous palladium complexes have emerged as powerful tools for carbon-carbon bond formation processes, such as Suzuki-Miyaura, Heck, Sonogashira, and Tsuji–Trost coupling reactions.[1-4] Despite of high efficiency, their practical applications are seriously restricted to the separation of soluble palladium complexes from the reaction systems and recycling of the expensive catalysts.[5] To address this problem, scientists have developed various immobilization methods to heterogenize palladium catalysts on solid supports.[6, 7] A number of organic or inorganic materials are employed as the support, ranging from organic polymers[8, 9], inorganic materials such as mesoporous silica[10, 11], zeolites[12], to magnetic nanoparticles[13]. However, although heterogenization allows easy separation and recovery, the heterogeneous feature often leads to more difficult contacts of reactants with catalytic active sites, resulting in inferior catalytic activities. Furthermore, the coordination ligand and surrounding environment of the metal center not only decide the steric and electronic properties, but also play crucial roles in the catalytic process.[14, 15] Well-established heterogenization strategies typically involve multi-functionalization steps and call for costly coordination ligands. Therefore, to combine the advantages of homogeneous and heterogeneous catalysis, efficient heterogenization strategies and versatile supports with industrial potential are still desired.

In general palladium catalytic systems, free base is often employed as an efficient additive. For instance, in the Tsuji–Trost coupling process which generates the allylation of a nucleophile with an allylic compound, both a palladium catalyst and a base should be included. The base promotes the activation of the nucleophile to attack the palladium intermediate species in the catalytic cycle.[16, 17] Although homogeneous palladium complexes have been immobilized through various methods, few studies reach the combination of bases with palladium complexes in heterogenization systems.[18, 19] By merging palladium species with bases (such as organic amines) on the same bifunctional solid surface, the accumulated multi-active sites should promote the dual interactions of reactive molecules. Therefore, a cooperative catalyst by combining a palladium complex and a base on one support is supposed to achieve excellent catalytic performance.[20, 21]

Recently, the intriguing nanomaterials, graphene and graphene oxide (GO),[22, 23] have attracted enormous studies in both academic and industrial fields for their remarkable properties.[24-26] Arising from the unique two-dimensional structures, huge surface area, and excellent dispersibility, GO has been demonstrated to be a versatile support for palladium nanocrystals or nanoparticles.[27-30] Remarkable catalytic performances have been observed of the hybrids as the catalytic reactions take place on the two-dimensional surface, thus internal diffusion would not be an issue. More importantly, the abundant oxygen-containing groups (mainly hydroxyls, carboxyls and epoxides) on the planar surfaces and edges of GO allow various chemical functionalizations.[31-33] The modification availability of GO provides great opportunities for anchoring coordination ligands and incorporation basic groups at the same time. So these characters reveal that GO possesses great potential as a desirable bifunctional support for combining palladium complexes and bases together.[34]

Hence, in the present study, we design a facile strategy to combine a palladium complex and an organic base on GO support as a cooperative catalyst for Tsuji–Trost allylation (Scheme 1). With $PdCl_2$ used as the precursor, the palladium-diamine complex is in situ synthesized and immobilized on GO by direct coordination (GO-2N-Pd). No extra ligand, such as triphenylphosphine (PPh_3), is needed for the developed palladium system. Mainly serving as an organic base, a tertiary amine is simultaneously immobilized on the support through a silylation process. The tertiary amine shows synergistic catalysis effect with the palladium-diamine complex and significantly promotes the activity for Tsuji–Trost allylation. Besides the high activity, the cooperative supported catalyst (GO-NEt_2-2N-Pd) can also be readily recovered and recycled for several times without reduction of the efficiency.

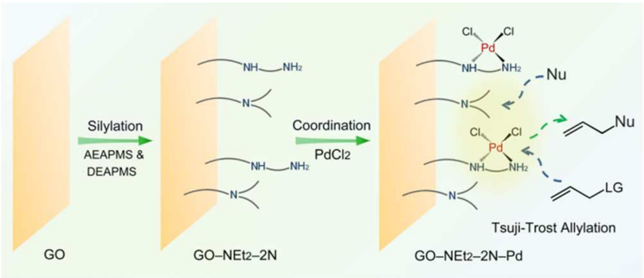

Scheme 1 Illustration for the synthetic methodology of GO-NEt_2-2N-Pd and Tsuji–Trost allylation catalyzed by the cooperative catalyst. Nu, nucleophile; LG, leaving group.

Experimental

Materials

[3-(diethylamino) propyl] trimethoxysilane (DEAPMS, 98%), allyl methyl carbonate (98%), palladium chloride ($PdCl_2$, 99%) and graphite powder (99.9%) were purchased from Sigma-Aldrich Chem. Co. (USA). Ethyl acetoacetate (99%), 3-(2-aminoethylamino) propyl trimethoxysilane (AEAPMS, 95%), dioxane (99%), triethylamine (98%), pyridine (99%), potassium carbonate (K_2CO_3, 99%) and Pd/C catalyst (5 wt% Pd) were purchased from Aladdin Reagent Co. (Shanghai, China). Other chemicals were of reagent grade and used as received.

Characterization

Fourier transform infrared (FTIR) spectra were measured with a Nicolet Nexus FTIR Spectrometer using the KBr pellet technique. X-ray photoelectron spectroscopy (XPS) measurements were performed on a PHI 1600 spectrometer with Al Kα radiation as an excitation source. Element analysis (EA) for nitrogen was performed on an Elementar Varioel element analyzer. Scanning electron microscopic (SEM) images and energy dispersive X-ray spectroscopy (EDS) element mapping analysis were recorded on the Hitachi Model S-4800 instrument. Transmission electron microscopic (TEM) images were determined using a JEM-2100F transmission electron microscope operating at 200 kV. The palladium contents were detected by inductively coupled plasma optical emission spectroscopy (ICP-OES, Vista-MPX). The catalytic results were determined by Agilent 6890N gas chromatography (GC) using a GC-FID system.

Preparation of GO

GO was prepared and purified by the typical Hummers method.[35] In brief, 10 g of natural graphite powder and 5 g of $NaNO_3$ were added into 230 mL of concentrated H_2SO_4 in an ice-bath with vigorous stirring. Then 30 g of $KMnO_4$ was gradually added into the mixture with the temperature controlled below 10 ^{o}C. The system was stirred at 35 ^{o}C for another 2 h. The temperature was raised to 98 ^{o}C after 460 mL of deionized water was slowly added. After 1 h stirring, the viscous mixture was diluted to 1400 mL with deionized water. Subsequently, a certain amount of 5% H_2O_2 was dropwise added until it turned to bright golden yellow. The mixture was filtered and washed three times with 5% aqueous HCl and hot deionized water, respectively. The GO product was further purified by 3 days of dialysis.

Synthesis of GO-NEt_2-2N and GO-NEt_2-2N-Pd

The prepared GO (5.0 mg mL^{-1}, 40 mL) was dispersed in 60 mL ethanol within a three necked flask, followed by ultrasonication for 0.5 h (25 W, 40 KHz). Subsequently, the flask was moved into a water bath at 78 ^{o}C. After being vigorously stirred for a few minutes, AEAPMS (117.1 mg, 0.5 mmol) was added into the suspension. 1 h later, 3 equivalents of DEAPTS (360.0 mg, 1.5 mmol) was dripped into the mixture. The mixture was stirred and refluxed for 12 h. After cooling to room temperatures, GO-NEt_2-2N was obtained by filtration and washing with ethanol three times, followed by freeze-drying. Preparation of GO-NEt_2-2N-Pd was processed as follows. GO-NEt_2-2N (300 mg) was dispersed in 60 mL water/ethanol (1:2, v/v). To anchor more palladium complexes, excessive amount of $PdCl_2$ (26.6 mg, 0.15 mmol) was added into the suspension. After ultrasonication for 15 min, the mixture was stirred at room temperatures for 24 h under an argon atmosphere. After the reaction, to recycle the un-immobilized palladium ions, the mixture was filtered and washed with 30 mL water/ethanol (1:2, v/v). The filtrate was recycled for further use. The filter cake was continuedly washed with ethanol and water multi times until no palladium ions were detected in the filtrate. The resulting sample was dried through a freeze-drying procedure.

Procedure for Tsuji–Trost Allylation

The catalytic reactions were conducted in a 10 mL Schlenk tube. In general, 43.5 mg of GO-NEt_2-2N-Pd (0.004 mmol Pd species) and 3.0 mmol of K_2CO_3 (418.8 mg) were dispersed in 5 mL of dioxane. Subsequently, 1.0 mmol of ethyl acetoacetate (131.5 mg) and 2.5 mmol of allyl methyl carbonate (296.2 mg) were added. The reaction mixture was then ultrasonicated for 15 min. After degassed with argon three times, the reaction mixture was heated to 70 ^{o}C using an oil bath and stirred for 5 h under an argon atmosphere. After cooling to room temperatures, sample was taken from the mixture and analyzed by GC. Repeated experiments were carried out for averaging data. For the control experiments, samples containing the same amount of palladium species (0.004 mmol) were employed as the catalyst.

Recycling Tests

For the recycling tests, the reactions were carried out under the same reaction conditions as described above. After the completion of each cycle, the reaction system was cooled to room temperatures. Then, the catalyst was recovered from the mixture by centrifugation and washed with dioxane three times, which was reused in the sequential cycles. K_2CO_3 was supplied at the beginning of each new cycle.

Results and discussion

Synthesis and Characterization of GO-NEt$_2$-2N-Pd

Owing to the modification diversity, GO provides an ideal platform to combine the palladium complex and organic amine together. As shown in Scheme 1, GO-NEt$_2$-2N-Pd is prepared through a facile synthetic methodology. In brief, to introduce the linkage for palladium and tether the tertiary amine, GO is first covalently modified with 3-(2-aminoethylamino) propyl trimethoxysilane (AEAPMS) and [3-(diethylamino) propyl] trimethoxysilane (DEAPMS) through a silylation process (named as GO-NEt$_2$-2N).[36] The immobilized DEAPMS mainly serves as an organic base, and AEAPMS is ready for the in situ synthesis and immobilization of the palladium complex. $PdCl_2$ is chosen as the palladium precursor. It should be noted that AEAPMS and DEAPMS are both inserted through a one-pot silylation reaction with the limited hydroxyl and carboxyl groups on GO. Considering the competition between them, samples with different proportions have been prepared. For the designed GO-NEt$_2$-2N-Pd, a molar ratio of 1:3 (AEAPMS : DEAPMS) was chosen to give the best catalytic performance.

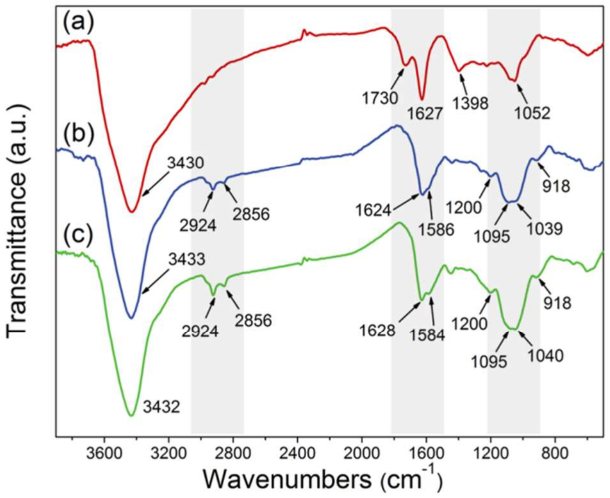

Fig. 1 FTIR spectra of (a) GO, (b) GO-NEt$_2$-2N, and (c) GO-NEt$_2$-2N-Pd.

Fig. 1 shows the Fourier transform infrared (FTIR) spectra of the pristine GO, GO-NEt$_2$-2N, and GO-NEt$_2$-2N-Pd. The characteristic absorptions of GO can be observed, including peaks at 3430 cm^{-1} for O–H in hydroxyl group coupled with absorbed water, 1730 cm^{-1} for C=O in carboxyl group, 1627 cm^{-1} for C=C in the aromatic ring, 1398 cm^{-1} for O–H in carboxyl group, and 1052 cm^{-1} for C–O in epoxide group.[37] Comparison studies on GO-NEt$_2$-2N and GO reveal additional peaks at 2924 and 2856 cm^{-1} attributed to C–H stretching vibrations from the silane chains of AEAPMS and DEAPMS. Due to overlapping absorption of absorbed water, the characteristic N–H stretching vibrations expected at around 3400 cm^{-1} is not clear. However, the appearance of an impregnate peak at 1586 cm^{-1} corresponding to bending vibrations of N–H and stretching vibrations of C–N at around 1200 cm^{-1} verify the existence of aminosilanes. The strong doublet at 1095 and 1039 cm^{-1} corresponding to characteristic absorption of Si–O–C&Si–O–Si provides more convincing evidence for the successful silanization of GO. The new peak at 918 cm^{-1} may be assigned to Si–OH vibrations arised from partial hydrolysis of the silane molecules.[38] As reported before, disappearance of the C=O peak at 1730 cm^{-1} was observed, suggesting silylation also occurs between the carboxyl groups and silane molecules.[36] No much difference can be observed with a further comparison of the spectra of GO-NEt$_2$-2N and GO-NEt$_2$-2N-Pd.

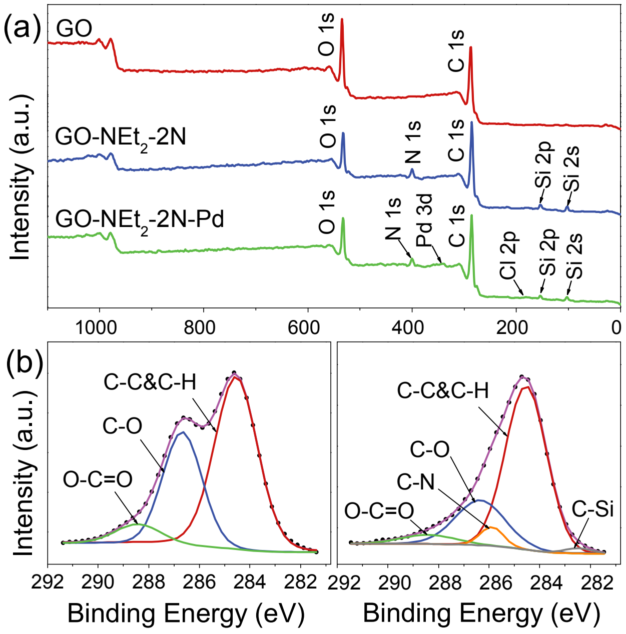

Fig.2 (a) Full range XPS Spectra of GO, GO-NEt$_2$-2N, and GO-NEt$_2$-2N-Pd. (b) High-resolution C 1s XPS spectra of GO and GO-NEt$_2$-2N-Pd.

X-ray photoelectron spectroscopy (XPS) is employed to investigate composition and bonding changes of the prepared samples. Fig. 2a presents the full range XPS spectra of GO, GO-NEt$_2$-2N, and GO-NEt$_2$-2N-Pd. As expected, the spectrum of GO shows only C and O peaks, with an O/C ratio of 0.37. The appearance of Si and N signals in the spectrum of GO-NEt$_2$-2N, along with the decrease of O/C ratio to 0.22 suggest the introduction of aminosilanes. More additional signals of Pd and Cl in GO-NEt$_2$-2N-Pd suggest the existence of the palladium complexes. Fig. 2b shows the high-resolution C 1s XPS spectra of GO and GO-NEt$_2$-2N-Pd. The spectrum of GO is split into three peaks at 284.5 eV, 286.76 eV and 288.5 eV, attributed to the C–C&C–H, C–O, and O–C=O, respectively.[39] Comparisons of the spectrum of GO-NEt$_2$-2N-Pd with GO show the appearance of C–N peak at 285.8 eV and C–Si peak at 282.5 eV. An obvious decrease of the peak at 286.6 eV corresponding to C–O–C and C–OH groups is also observed, indicating the conversion of C–OH into Si–O–C bonds in the silylation process.[40]

To verify the synthesis of the palladium-diamine complex, further study is carried out on the N 1s and Pd 3d XPS spectra. As shown in Fig. 3a, the N 1s XPS spectra of GO-NEt$_2$-2N and GO-NEt$_2$-2N-Pd are consisted of two peaks at around 399.0 eV and 400.9 eV, corresponding to bonding energy of C–NH–C&C–NH$_2$ and C–N, respectively. After the addition of PdCl$_2$, the C–NH–C&–NH$_2$ band shifts to a higher bonding energy (from 398.9 to 399.2 eV). This phenomenon should be induced by the donor-acceptor interaction between the nitrogen and palladium atoms.[41] According to the peak areas of C–NH–C&C–NH$_2$ and C–N, the ratio of inserted AEAPMS and DEAPMS is about 1.5:1. In the XPS spectrum of GO-NEt$_2$-2N-Pd, the Pd 3d core level region displays a Pd 3d$_{5/2}$ peak at 337.8 eV and Pd 3d$_{3/2}$ peak at 343.3 eV, which corresponds to the bonding energy of Pd(II) species (Fig. 3b).[42] Considering the limitation of surface characterization by XPS, inductively coupled plasma optical emission spectroscopy (ICP-OES) is employed to test the palladium content. The amount of palladium is calculated to be 0.092 mmol g^{-1} (0.98 wt %) (Table S1, ESI†). With the help of elemental analysis (EA), the amount of inserted N is determined to be 2.94 mmol g^{-1} (4.11 wt %). Thus, the amount of inserted Si is calculated to be 1.84 mmol g^{-1} (5.15 wt %), consisting of 1.10 mmol g^{-1} of AEAPMS and 0.74 mmol g^{-1} of DEAPMS, respectively.

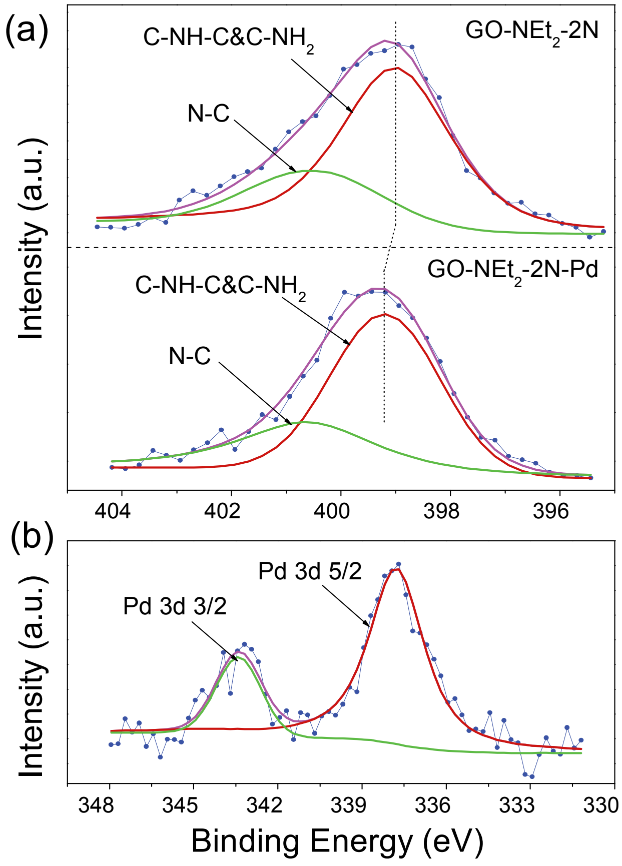

Fig. 3 (a) N 1s XPS spectra of GO-NEt$_2$-2N and GO-NEt$_2$-2N-Pd. (b) Pd 3d XPS spectrum of GO-NEt$_2$-2N-Pd.

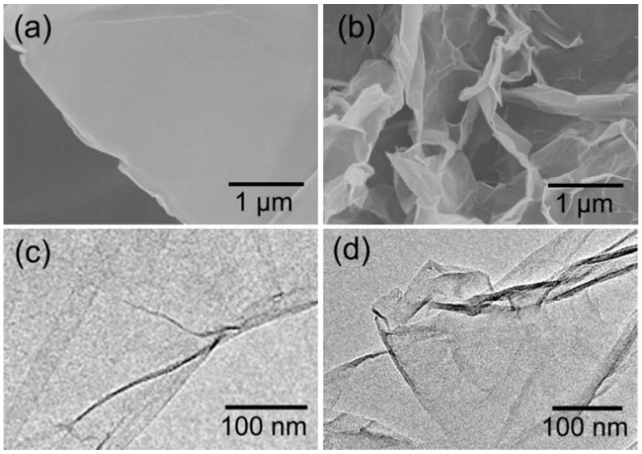

Fig. 4 SEM and TEM images of (a) (c) GO and (b) (d) GO-NEt$_2$-2N-Pd.

The microstructure and morphology of the samples are measured by means of scanning electron microscopy (SEM) and transmission electron microscopy (TEM) (Fig. 4). SEM and TEM images of GO exhibit the typical exfoliated nanostructure with a rather flat and smooth sheet-like morphology (Fig. 4a, b). More crumpled wrinkles are observed for the resulting GO-NEt$_2$-2N-Pd, which should be attributed to thermal treatments and chemical modifications (Fig. 4c, d). However, it still keeps the two-dimensional planar features of GO, and the microstructure of the support is not destroyed. This crumpling morphological feature may have potential advantages to facilitate mass transfer in the catalytic process, because the reactive species can readily access and leave the active sites on both sides of the two-dimensional graphene sheets.[43] Further study by quantitative energy dispersive X-ray spectroscopy (EDS) mapping shows that Si, Cl, Pd elements can be homogeneously distributed on the overall GO surface (Fig. 5). On one hand, it confirms the efficient immobilization of the palladium complexes; on the other hand, it reveals a uniform distribution of the catalytic sites on the GO surface.

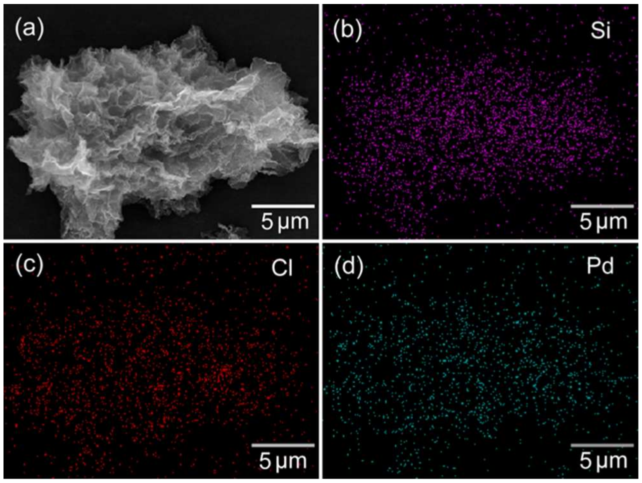

Fig. 5 (a) SEM image of GO-NEt$_2$-2N-Pd and corresponding quantitative EDS element mapping of (b) Si, (c) Cl and (d) Pd.

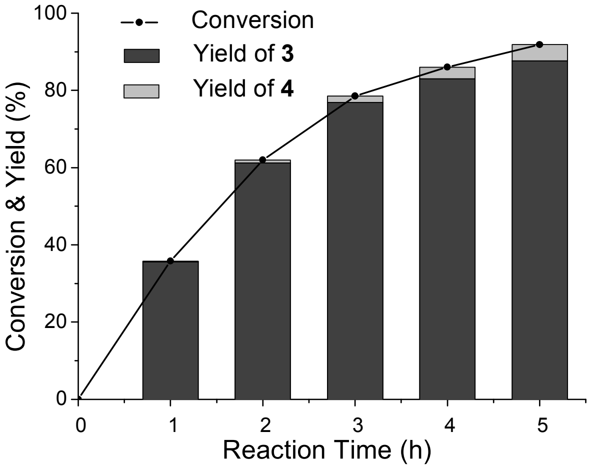

Fig. 6 Curve of conversion and yield versus reaction time for the Tsuji–Trost allylation process.

Catalytic Tsuji–Trost Allylation

Tsuji–Trost allylation of allyl methyl carbonate (**1**) with ethyl acetoacetate (**2**) was examined as a model catalytic reaction for the prepared GO-NEt$_2$-2N-Pd. The reaction was performed in dioxane at 70 °C by using K_2CO_3 as an external base (Scheme 2). Due to the double nucleophilic sites of **1**, mono-allylation product (**3**) and di-allylation product (**4**) were both generated. As shown in Fig. 6, the allylation proceeded smoothly with a very low Pd-loading of 0.4 mol %). Both the conversion and yield increased with the reaction time. At the beginning of the reaction, trace amounts of **4** could be detected. The yield of **4** slightly increased with the proceeding of the reaction, which suggested further allylation of **3** occurred at the same time. The conversion reached up to 91.85% in 5 h, with a final turnover frequency (TOF) of 46.0 h^{-1}. No by-product was obtained, and the yields of **3** and **4** were detected to be 87.67% and 4.18%, respectively.

To investigate the effective component, a series of control experiments were conducted. The results are summarized in Table 1. When no catalyst or GO-NEt$_2$-2N was used, hardly any conversion occurred, indicating the reaction cannot proceed with the absence of palladium catalytic component (Entry 1 and 2). Probably due to the absence of coordination ligands, treatment of the homogeneous $PdCl_2$ with **1** and **2** also gave a poor conversion and yield for **3** (Entry 3). By being immobilized on GO, GO-2N-Pd exhibited catalytic efficiency for the resulting in a 44.52% conversion and 44.03% yield for **3** (Entry 4). Reactions with addition of free triethylamine were out. Comparison of Entry 5 and 6 with Entry 3 and 4 reveals a small amount of free tertiary amine can slightly accelerate the conversion to **3**. By immobilizing equivalent tertiary amine on GO-2N-Pd, the cooperative supported catalyst (GO-NEt$_2$-2N-Pd) achieved a significantly promoted result, with yields of 87.67% and 4.18% for **3** and **4**, respectively (Entry 7). So anchoring of tertiary amine on the support presents an obvious enhanced effect for the conversion. Commercial Pd/C catalyst was also employed as a control (Entry 8). With equivalent amount of palladium species, yields of **3** and **4** were examined to be 54.34% and 0.59%, respectively, which is much lower than that of GO-NEt$_2$-2N-Pd. Palladium immobilized on tertiary amine functionalized GO was also prepared (GO-NEt$_2$-Pd). The Pd content was detected to be 0.24 wt %, which is much lower than that of GO-2N-Pd. By employing a large amount of catalyst containing equivalent palladium, a comparable activity with GO-2N-Pd was obtained (Entry 9). The results reveal very small amount of inserted tertiary amine also coordinates with palladium to form palladium-tertiaryamine complex, and the plenty tertiary amine accounts for the good catalytic conversion of GO-NEt$_2$-Pd. Considering the much lower catalytic activity compared with GO-NE$_2$-2N-Pd, the palladium-diamine complex should be a much more effective species than palladium-tertiaryamine complex. The above results indicate palladium complexes are the critical catalytic component for the Tsuji–Trost allylation, and immobilized tertiary amine presents an obvious promoted effect for the conversion.

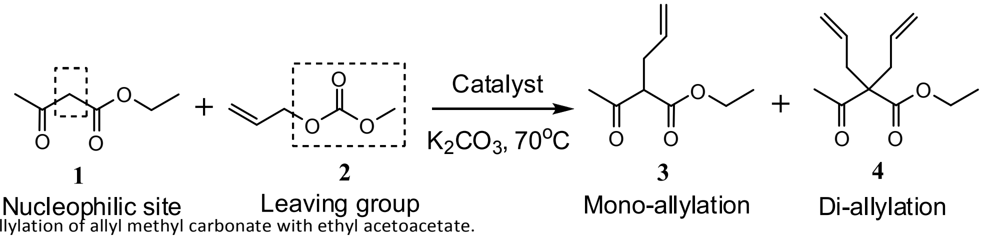

Scheme 2 Tsuji–Trost allylation of allyl methyl carbonate with ethyl acetoacetate.

Table 1 Tsuji–Trost reaction catalyzed by various Pd catalysts.[a]

Entry	Catalyst	Conversion (%) [b]	Yield (%) [b] 3	Yield (%) [b] 4
1	None	2.70	0	0
2	GO-NEt$_2$-2N [c]	4.03	0	0
3	PdCl$_2$	6.43	2.82	0
4	GO-2N-Pd	44.52	44.03	0.49
5	PdCl$_2$ + Triethylamine [d]	10.44	9.20	0
6	GO-2N-Pd + Triethylamine [d]	50.83	50.11	0.72
7	GO-NEt$_2$-2N-Pd	91.85	87.67	4.18
8	Pd/C [e]	54.93	54.34	0.59
9	GO-NEt$_2$-Pd [f]	46.89	46.39	0.50

[a] General conditions: **1** (1.0 mmol), **2** (2.5 mmol), K_2CO_3 (3.0 mmol), catalyst (Pd: 0.004 mmol), dioxane (5.0 mL), 70 °C, 5 h. [b] Calibrated conversion and yield determined by gas chromatography (GC). [c] 43.5 mg of GO-NEt$_2$-2N (the same weight with GO-NEt$_2$-2N-Pd). [d] Triethylamine (0.04 mmol). [e] 8.5 mg of Pd/C catalyst. [f] 177.4 mg of GO-NEt$_2$-Pd.

Considering the promotion effect on the catalytic result, further study was carried out to get a better insight into the role of the tertiary amine. The investigation was conducted by preparing a series of samples with different amount of DEAPMS (Table 2). Compared with GO-2N-Pd, an obvious increase of the conversion and yield for **3** and **4** was observed with 1 equivalent (equiv.) of DEAPMS added, which suggests the presence of tertiary amine facilitates the conversion of the allylation process (Entry 1-2). With more DEAPMS immobilized on GO, the cooperative supported catalyst achieved a further increase of conversion and yield (Entry 3-4). The catalytic result of commercial Pd/C catalyst above shows that Pd(0) should also be an effective species towards the reaction. Additional experiments on GO-NEt$_2$-2N supported palladium catalysts indicate nanoparticle size of Pd(0) is also an important factor affecting the catalytic results (see ESI† for details). To exclude this factor, the used catalysts were detected by TEM. As shown in Fig. S1, all of the samples exhibit few nanoparticles with comparable size agglomerated on the GO surface (ESI†). No much difference can be seen between them. Considering the small amount and comparable size, the influence of nanoparticle size on the catalytic results can be ignored. Therefore, the results document the role of immobilized tertiary amine as a synergistic effective unit with the palladium complex, and it significantly promotes the catalytic activity for the Tsuji–Trost allylation.

Table 2 Influence of the amount of DEAPMS on the catalytic results.

Entry	Catalyst	Conversion (%) [b]	Yield (%) [b] 3	Yield (%) [b] 4
1	0 equiv. DEAPMS	44.52	44.03	0.49
2	1 equiv. DEAPMS	72.12	70.72	1.40
3	2 equiv. DEAPMS	82.23	79.40	2.83
4	3 equiv. DEAPMS	91.85	87.67	4.18

[a] General conditions: **1** (1.0 mmol), **2** (2.5 mmol), K_2CO_3 (3.0 mmol), catalyst (0-3 equiv. of DEAPMS immobilized on GO, Pd: 0.004 mmol) , dioxane (5.0 mL), 70 °C, 5 h. [b] Calibrated conversion and yield determined by GC.

The impact of free base on the conversion and selectivity for mono- and di- allylation products was also investigated. Table 3 summarizes the results of the reaction by employing various inorganic and organic bases. Typically, in homogeneous system, the plenty free triethylamine or pyridine would coordinate to the palladium center, which leads to structure changes of the metal active center and thus cause deactivation of the catalyst. Therefore, organic bases show extremely low efficiency towards the reaction with some by-products (Entry 1-2), which is not suitable for the reaction. However, inorganic bases can yield from low to excellent performances (Entry 3-5). The differences might be related to their alkalinity. Bases with weak alkalinity tend to give a low conversion, but a favor of mono-allylation products. Just the opposite, bases with strong alkalinity achieves an excellent conversion, but a mixture of mono- and di- allylation products are both obtained. Taken together, K_2CO_3 is a reasonable choice as an effective and selective additive for the reaction.

Table 3 Influence of the free base on the catalytic results. [a]

Entry	Base	Conversion (%) [b]	Yield (%) [b] 3	Yield (%) [b] 4
1	Triethylamine	6.21	1.74	0
2	Pyridine	4.90	0.88	0
3	Li_2CO_3	6.36	6.36	0
4	K_2CO_3	91.85	87.67	4.18
5	Cs_2CO_3	93.80	78.11	15.69

[a] General conditions: **1** (1.0 mmol), **2** (2.5 mmol), GO-NEt$_2$-2N-Pd (Pd: 0.004 mmol) , base (3.0 mmol), 70 °C, 5 h. [b] Calibrated conversion and yield determined by GC.

After each reaction, the catalyst could be easily recovered from the mixture by centrifugation and ready for reuse after washing with dioxane three times. The reusability and stability of GO-NEt$_2$-2N-Pd was examined by recycling tests. As seen in Fig. 7, GO-NEt$_2$-2N-Pd showed excellent catalytic performance upon reuse. It could maintain the high activity for at least five cycles without reduction of catalytic activity. After the reaction, GO-NEt$_2$-2N-Pd could be readily recovered by a centrifugation procedure. Metal leaching was examined by ICP analysis, and no detectable palladium ions were detected in the reaction solution, revealing the robust immobilization of palladium. It is worth to notice that the catalyst showed a slightly enhanced conversion and yield in the first few recycles compared with the fresh one. Thus, we tested the recycled catalyst after five-cycle reuse. SEM image showed the recycled catalyst still kept the sheet-like morphology with some indistinct particles (Fig. S2, ESI†). TEM detection verified the attachment of much more nanoparticles on the GO surface compared with Fig. S1 (Fig. S3, ESI†). XPS analysis revealed the appearance of new small Pd $3d_{5/2}$ peak at 335. 5 eV and Pd $3d_{3/2}$ peak at 340.6 eV, corresponding to Pd(0) (Fig. S4, ESI†). Therefore, a small amount of Pd(II) converted into Pd(0) nanoparticles with the proceeding of the recycling tests. As Pd(0) is also an effective species for the reaction, the agglomerated nanoparticles can not only prevent the leaching of palladium, but also account for the excellent reusability of the catalyst.[42]

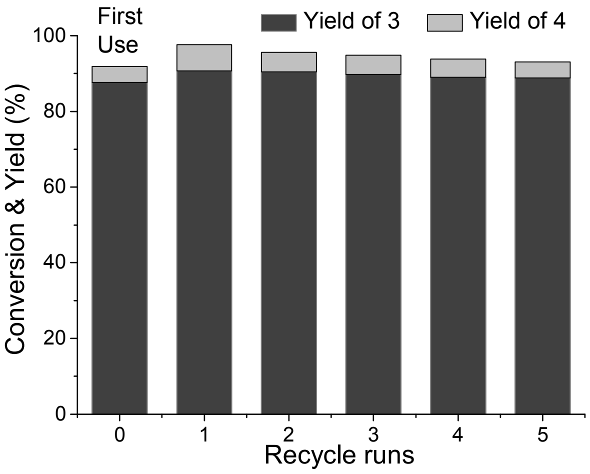

Fig. 7 Catalyst recycling runs for the Tsuji–Trost allylation.

The excellent catalytic performance of GO-NEt$_2$-2N-Pd might be ascribed to synergistic catalysis effect, remarkable support properties, and robust immobilization interaction. As illustrated in Fig. 8,[44] in the allylation cycle, the allyl group of ethyl acetoacetate (**2**) first coordinates with the palladium centre, and then the leaving group expels with inversion of configuration, forming (π-allyl) palladium species. At the same time, the neighbouring tertiary amine pulls the nucleophile (**1**) to the GO surface by donating a pair of electrons and activates the nucleophile along with the K_2CO_3 in the solution. Then, the nucleophile attacks the palladium intermediate, followed by the detachment of the palladium and resulting in the formation of the allylation product (**3**). In the combined catalytic system, the immobilized palladium complexes act as the essential catalytic center. The tertiary amine promotes the reaction by anchoring and activating the nucleophile. So synergistic catalysis effect[20] induced by the two effective species ensures the smooth proceeding of the reaction. In addition, due to the multi-functional groups existing on the GO support, the heterogenized catalyst may present some pseudo-homogeneous characters in the reaction solution. The two-dimensional structure and large surface area of the GO support also make sure that the reactive species can facilely reach or leave the catalytic active sites with limited mass transfer resistance. What's more, given the instability of catalytic species is often caused by the formation of inactive multinuclear species or self-agglomeration,[45] especially for this metal complex and organic molecule cooperative system. So owing to site isolation effect[46] by robust immobilization interaction, it can prevent the formation of inactive species and self-quenching in the catalytic process.

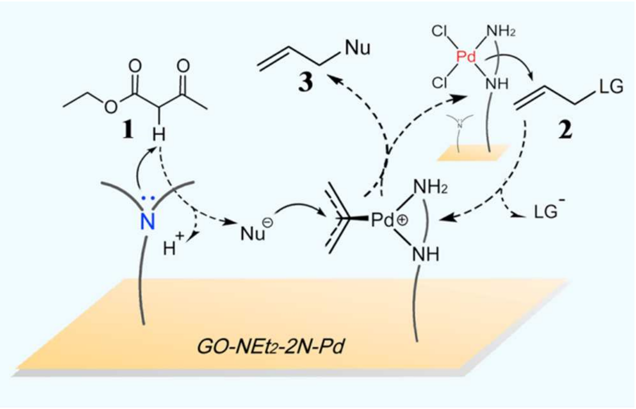

Fig. 8 Catalytic mechanism of Tsuji–Trost allylation process catalyzed by GO-NEt$_2$-2N-Pd. Nu, nucleophile; LG, leaving group.

Conclusions

In conclusion, we have facilely prepared a cooperative supported catalyst by simultaneously immobilizing a palladium-diamine complex and a tertiary amine on GO support. With a very low Pd-loading, the catalyst presents excellent catalytic performance towards Tsuji–Trost allylation. The tertiary amine is determined as a synergistic effective unit with the palladium-diamine complex and significantly promotes the catalytic efficiency. This work has demonstrated a facile, green and economical strategy to merge an organic amine with a metal complex on GO, which provides an ideal platform to combine them together. The strategy may open the door to the combination of transition metal catalysis and amine catalysis in graphene-based heterogenization systems, and more academic and industrial applications are anticipated.

Acknowledgements

This study was supported by the National Natural Science Funds for Excellent Young Scholars (no. 21222608), Research Fund of the National Natural Science Foundation of China (no. 21106099), Foundation for the Author of National Excellent Doctoral Dissertation of China (no. 201251), the Tianjin Natural Science Foundation (no. 11JCYBJC01700) and the Programme of Introducing Talents of Discipline to Universities (no. B06006).

Notes and references

[a] State Key Laboratory of Chemical Engineering, School of Chemical Engineering & Technology, Collaborative Innovation Center of Chemical Science and Engineering, Tianjin University, Tianjin, 300072, China.

Electronic Supplementary Information (ESI) available: [TEM images of used catalysts with different amount of DEAPMS, ICP test result of GO-NEt$_2$-2N-Pd are included. SEM, TEM, and XPS analysis of recycled GO-NEt$_2$-2N-Pd, as well as the additional experiments are also involved.] See DOI: 10.1039/b000000x/

1. F.-S. Han, *Chem. Soc. Rev.*, 2013, **42**, 5270-5298.

2. R. Chinchilla and C. Nájera, *Chem. Rev.*, 2013, **114**, 1783-1826.
3. X. Chen, K. M. Engle, D.-H. Wang and J.-Q. Yu, *Angew. Chem. Int. Ed.*, 2009, **48**, 5094-5115.
4. S. C. Sau, S. Santra, T. K. Sen, S. K. Mandal and D. Koley, *Chem. Commun.*, 2012, **48**, 555-557.
5. M. Pagliaro, V. Pandarus, R. Ciriminna, F. Béland and P. Demma Carà, *ChemCatChem*, 2012, **4**, 432-445.
6. M. Lamblin, L. Nassar-Hardy, J.-C. Hierso, E. Fouquet and F.-X. Felpin, *Adv. Synth. Catal.*, 2010, **352**, 33-79.
7. Á. Molnár, *Chem. Rev.*, 2011, **111**, 2251-2320.
8. H.-J. Cho, S. Jung, S. Kong, S.-J. Park, S.-M. Lee and Y.-S. Lee, *Adv. Synth. Catal.*, 2014, **356**, 1056-1064.
9. B. Basu, S. Das, P. Das, B. Mandal, D. Banerjee and F. Almqvist, *Synthesis-Stuttgart*, 2009, 1137-1146.
10. V. Polshettiwar, C. Len and A. Fihri, *Coordin. Chem. Rev.*, 2009, **253**, 2599-2626.
11. B. Basu and S. Paul, *Appl. Organomet. Chem.*, 2013, **27**, 588-594.
12. Z. Guan, J. Hu, Y. Gu, H. Zhang, G. Li and T. Li, *Green Chem.*, 2012, **14**, 1964-1970.
13. J. Yang, D. Wang, W. Liu, X. Zhang, F. Bian and W. Yu, *Green Chem.*, 2013, **15**, 3429-3437.
14. Z. Wu, F. Berhal, M. Zhao, Z. Zhang, T. Ayad and V. Ratovelomanana-Vidal, *ACS Catal.*, 2013, **4**, 44-48.
15. Y. Yang and S. L. Buchwald, *J. Am. Chem. Soc.*, 2013, **135**, 10642-10645.
16. J. T. Mohr and B. M. Stoltz, *Chem. – Asian J.*, 2007, **2**, 1476-1491.
17. H. Noda, K. Motokura, A. Miyaji and T. Baba, *Angew. Chem.*, 2012, **124**, 8141-8144.
18. A. T. Dickschat, F. Behrends, S. Surmiak, Wei, H. Eckert and A. Studer, *Chem. Commun.*, 2013, **49**, 2195-2197.
19. I. Ibrahem, G. Ma, S. Afewerki and A. Córdova, *Angew. Chem.*, 2013, **125**, 912-916.
20. A. E. Allen and D. W. C. MacMillan, *Chem. Sci.*, 2012, **3**, 633-658.
21. M. Ikeda, Y. Miyake and Y. Nishibayashi, *Angew. Chem. Inter. Ed.*, 2010, **49**, 7289-7293.
22. A. K. Geim and K. S. Novoselov, *Nat. Mater.*, 2007, **6**, 183-191.
23. D. Chen, H. Feng and J. Li, *Chem. Rev.*, 2012, **112**, 6027-6053.
24. K. P. Loh, Q. Bao, G. Eda and M. Chhowalla, *Nat. Chem.*, 2010, **2**, 1015-1024.
25. L. P. Biro, P. Nemes-Incze and P. Lambin, *Nanoscale*, 2012, **4**, 1824-1839.
26. X. Huang, X. Y. Qi, F. Boey and H. Zhang, *Chem. Soc. Rev.*, 2012, **41**, 666-686.
27. G. M. Scheuermann, L. Rumi, P. Steurer, W. Bannwarth and R. Mülhaupt, *J. Am. Chem. Soc.*, 2009, **131**, 8262-8270.
28. S. Moussa, A. R. Siamaki, B. F. Gupton and M. S. El-Shall, *ACS Catal.*, 2011, **2**, 145-154.
29. A. Shaabani and M. Mahyari, *J. Mater. Chem. A*, 2013, **1**, 9303-9311.
30. H. Y. Li, S. Y. Gan, D. X. Han, W. G. Ma, B. Cai, W. Zhang, Q. X. Zhang and L. Niu, *J. Mater. Chem. A*, 2014, **2**, 3461-3467.
31. D. R. Dreyer, S. Park, C. W. Bielawski and R. S. Ruoff, *Chem. Soc. Rev.*, 2010, **39**, 228-240.
32. M. Quintana, E. Vazquez and M. Prato, *Acc. Chem. Res.*, 2012, **46**, 138-148.
33. T. Kuila, S. Bose, A. K. Mishra, P. Khanra, N. H. Kim and J. H. Lee, *Prog. Mater. Sci.*, 2012, **57**, 1061-1105.
34. S. Sabater, J. A. Mata and E. Peris, *ACS Catal.*, 2014, **4**, 2038-2047.
35. W. S. Hummers and R. E. Offeman, *J. Am. Chem. Soc.*, 1958, **80**, 1339-1339.
36. H. Gaspar, C. Pereira, S. L. H. Rebelo, M. F. R. Pereira, J. L. Figueiredo and C. Freire, *Carbon*, 2011, **49**, 3441-3453.
37. M. Acik, G. Lee, C. Mattevi, M. Chhowalla, K. Cho and Y. J. Chabal, *Nat. Mater.*, 2010, **9**, 840-845.
38. P. Ma, Kim, Jang-Kyo, B. Tang, *Carbon*, 2006, **44**, 3232.
39. S. Kim, S. Zhou, Y. Hu, M. Acik, Y. J. Chabal, C. Berger, W. de Heer, A. Bongiorno and E. Riedo, *Nat. Mater.*, 2012, **11**, 544-549.
40. Q. S. Zhao, Y. Li, R. Liu, A. Chen, G. L. Zhang, F. B. Zhang and X. B. Fan, *J. Mater. Chem. A*, 2013, **1**, 15039-15045.
41. A. B. Dongil, B. Bachiller-Baeza, A. Guerrero-Ruiz and I. Rodríguez-Ramos, *J. Catal.*, 2011, **282**, 299-309.
42. G. Ding, W. Wang, T. Jiang and B. Han, *Green Chem.*, 2013, **15**, 3396-3403.
43. J. Ji, G. Zhang, H. Chen, S. Wang, G. Zhang, F. Zhang and X. Fan, *Chem. Sci*, 2011, **2**, 484-487.
44. B. M. Trost, T. Zhang and J. D. Sieber, *Chem. Sci.*, 2010, **1**, 427-440.
45. C. E. Song, *Annu. Rep. Prog. Chem., Sect. C*, 2005, **101**, 143-173.
46. R. J. Trovitch, N. Guo, M. T. Janicke, H. Li, C. L. Marshall, J. T. Miller, A. P. Sattelberger, K. D. John and R. T. Baker, *Inorg. Chem.*, 2010, **49**, 2247-2258.

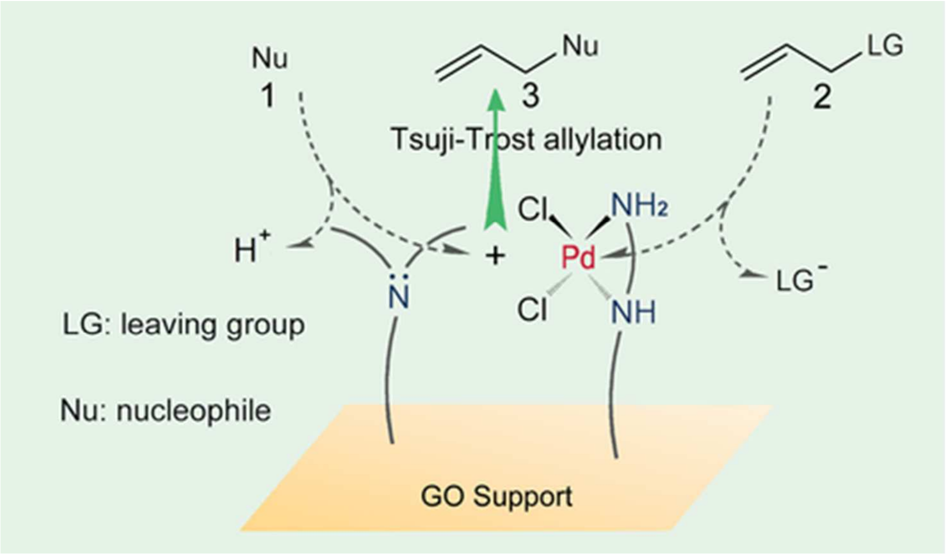

A palladium complex and a tertiary amine are combined on graphene oxide as a promoted and recyclable catalyst for Tsuji-Trost allylation
39x23mm (300 x 300 DPI)